Acta Geophysica (2021) 69:2363–2376
https://doi.org/10.1007/s11600-021-00667-6

RESEARCH ARTICLE - HYDROLOGY

Separation of surface flow from subsurface flow in catchments using runoff coefficient

A. Afshar Ardekani[1] · T. Sabzevari[1] · A. Torabi Haghighi[2] · A. Petroselli[3]

Received: 16 May 2021 / Accepted: 22 August 2021 / Published online: 17 September 2021

Abstract
Separating surface flow (SF) from subsurface flow (SSF) based on direct runoff measurements in river gauges is an important issue in hydrology. In this study, we developed a simple and practical method, based on runoff coefficient (RC), for separating SF from SSF. RC depends mainly on soil texture, land use and land cover, but we also considered the effect of slope and rainfall intensity. We assessed our RC-based method for three different soil types by comparing the value obtained with laboratory rainfall simulator data. The correlation coefficient between observed and calculated data exceeded 0.93 and 0.63 when estimating SF and SSF, respectively. The method was then used to separate SF and SSF in two catchments (Heng-Chi and San-Hsia) in Northern Taiwan, and the results were compared with those produced by the geomorphological instantaneous unit hydrograph (GIUH) model. Test revealed that, if RC is calculated accurately, the proposed method can satisfactorily separate SF from SSF at catchment scale.

Keywords Surface flow · Subsurface flow · Separation · Runoff coefficient

Introduction

Estimating direct runoff is important in flood risk assessment and in the design of hydraulic structures such as diversion and storage dams. In general, total runoff occurring in streams consists of three components: surface runoff, subsurface flow, and base flow. The sum of surface runoff and subsurface flow is commonly defined as direct runoff.

Surface runoff (SF) is usually the most important of such three components. Many rainfall-runoff models have been proposed to compute the surface flow of ungauged catchments (Menberu et al. 2014, Sabzevari 2017; Keshtkaran et al. 2018; Petroselli et al. 2020a, b; Dehghanian et al. 2020).

However, in hilly catchments with very permeable soil or dense vegetation cover, the rate of infiltration is high and can lead to rapid subsurface flow. In such catchments, subsurface flow can enter streams at the lower part of hillslopes and contribute effectively to direct flow (Singh 1988; Sabzevari et al. 2013).

The underground flow can be slow or quick. The quick underground flow is often called saturated subsurface flow (SSF), and it usually occurs near the soil surface, eventually entering the streams. Slow underground flow is generally a source of groundwater recharge. It is formed through the infiltration of water into deeper layers of the soil and eventually enters rivers as base flow (BF).

Based on the Dunne–Black runoff mechanism, the lower soil layers are saturated by SSF, which eventually joins surface flow (SF) entering the streams (Chow et al. 1988). To separate SF from SSF, the complicated interactions of saturated and unsaturated zones in soil must be determined. Several previous studies have attempted to separate SF from SSF, but this topic still needs further investigation (Hursh et al. 1941; Wels et al. 1991; Johst et al. 2013).

Harris et al. (1995) proposed a hydrograph separation method for runoff source modeling based on continuous

Communicated by Dr. Senlin Zhu (ASSOCIATE EDITOR), Dr. Michael Nones (CO-EDITOR-IN-CHIEF).

✉ T. Sabzevari
t_sabzevari@iauest.ac.ir; tooraj.sabzevari@gmail.com

[1] Department of Civil Engineering, Islamic Azad University, Estahban Branch, Fars, Iran

[2] Water, Energy and Environmental Engineering Research Unit, University of Oulu, Oulu, Finland

[3] Department of Economics, Engineering, Society and Business Organization (DEIM), Tuscia University, Via S. Camillo de Lellis snc, 01100 Viterbo, VT, Italy

open system isotope mixing, using a variable source area and three isotopic reservoirs. They examined time-dependent contributions of SF and SSF to total streamflow, and estimated parameters for determining the saturated area fraction-streamflow, and saturated area-subsurface water storage relationships (Harris et al. 1995).

A stable environmental isotope was used by Tekeli and Şorman (2003) to investigate the rainfall-runoff relationship and to separate SF from SSF in hydrographs, based on analysis of water samples from rainfall, runoff (total discharge), springs (subsurface flows), and wells (groundwater) in the Guvenc Basin, Turkey. Through this approach, they successfully determined the contribution of SSF originating from various sublayers.

Foks et al. (2019) used an optimal hydrograph separation technique based on a two-parameter recursive digital filter and specific conductance mass-balance constraints to estimate the base flow contribution to observed flow in river gauges.

Some previous studies of SSF at hillslope scale have used existing methods based on the Dupuit–Forchheimer approach, Boussinesq equation, or numerical solution of complex three-dimensional equations (e.g., Troch et al. 1993; Chen et al. 1994a, b). Numerical methods give good accuracy, but most hydrologists want simpler methods. Some hydrological models have also been used to estimate SSF (Robinson and Sivapalan 1996; Lee and Chang 2005; Sabzevari et al. 2013; Sabzevari and Noroozpour 2014).

Lee and Chang (2005) developed the geomorphological instantaneous unit hydrograph (GIUH) model for predicting SSF. Surface and subsurface travel time are the most important parameters in the GIUH model. Subsurface travel time is a function of overland length and slope and soil characteristics, e.g., hydraulic conductivity and porosity. Lee and Chang (2005) used the GIUH model to separate SF and SSF in the Heng-Chi basin, Taiwan.

Sabzevari et al. (2013) modified the Lee and Chang (2005) model by calculating the SSF hydrograph of the catchment through convoluting the subsurface GIUH model in the infiltration hyetograph. In their modified version, a more accurate saturation model was used to predict SF and SSF according to the Dunne–Black mechanism. Sabzevari et al. (2013) applied the modified model in the Kasilian catchment, Iran, to separate SF and SSF.

Sabzevari and Noroozpour (2014) examined the role of hillslope shape and profile curvature on SF and SSF in complex hillslopes and applied a new complex saturation model to separate the saturation region. They used the model to estimate SSF in a small basin, No. 125 in Walnut Gulch, Arizona, USA.

The theory of Sabzevari et al. (2013) was used by Petroselli (2020) that generalized the EBA4SUB rainfall-runoff model (Piscopia et al. 2015; Petroselli and Grimaldi 2018; Petroselli et al. 2020a, b), originally developed only for SF estimation. In such generalization, employing the Width Function Based IUH framework, the subsurface flow process was introduced, in doing so allowing the model application to both Hortonian and Dunne–Black runoff formation mechanisms.

Several studies have been presented on the separation of surface and subsurface flow from runoff hydrographs (Hursh and Brater 1941; Wels et al. 1991; Johst et al. 2013). Lee et al. (2015) introduced a new method to estimate the runoff coefficient through the infiltration analysis based on the comparative results of the existing runoff coefficient method. The effect of rainfall intensity and soil characteristics on runoff coefficient was also analyzed by the FFC-COBRA model and effective rainfall separation method based on NRCS CN. This result showed that the runoff coefficient in this study is in the range of runoff coefficient and the range of runoff coefficient and over the upper limit of 0.10 ~ 0.22 at 'forest, etc.' from ASCE.

Johst et al. (2013) studied a 31 ha headwater basin in Western Germany to separate the surface flow and subsurface flow from runoff hydrograph. In this study, the contribution of infiltration excess and saturation overland flow and matrix and preferential flow has been assessed along a deeply incised channel of 300 m length. Measurable parameters and simple algorithms were used to assess the flow rate of the different runoff components. The results showed that during wet conditions, the subsurface flow rates exceed the surface flow rates tremendously.

Laboratory physical models are commonly used to validate the results of SF and SSF estimation models. Essig et al. (2009) devised a laboratory setup to separate deep flow and surface flow for sloping surfaces. The equipment consisted of a rainfall simulator device with length 1.52 m and width 1.22 m and a soil box with a depth 78 cm, which was equipped to measure SSF and the SF separately by two weirs. In Essig et al. (2009), the separation between SF and SSF was also modeled by the Hydrus 2D (numerical) model for different slopes up to 10 degrees, and the results were compared.

The runoff coefficient (RC) is often used to separate the amount of excess rainfall from infiltration in many hydrological models (e.g., the rational method), in doing so trying to express the relationship between SF and SSF. The RC value indicates the ratio of surface runoff depth to total rainfall depth. Based on RC values, the surface runoff depth and infiltration depth can be determined (Kim and Shin 2018; Kim et al. 2016).

Indeed literature shows that RC depends on factors such as soil type and land use, slope and rainfall rate. In this study, we developed a new method for separating SF and SSF in catchments by investigating the effect of slope and rainfall intensity on RC. The most important innovation of this study is that the separation of SF from SSF is based only on RC. We verified the method using laboratory data in the hillslope dimension. Finally, we tested the separation of SF and SSF for two catchments (Heng-Chi and San-Hsia) in northern Taiwan and compared the modeled results with observed direct runoff.

The main classification of the sections of this article is as follows: In the first part, the equations of separation of surface and subsurface flow are presented, and then the effect of rainfall intensity and slope on surface flow is investigated. In the next section, the results of two laboratory models for measuring surface and subsurface flow are presented, and the observed runoff coefficients and the calculated runoff coefficient are evaluated. Finally, the proposed method for two catchments in Taiwan is evaluated.

Materials and methods

Separation of surface flow from subsurface flow

The amount of rainfall or liquid precipitation (P) falling on a hillslope (Fig. 1) can be calculated from the sum of surface runoff (R) and infiltration (F):

$$P = F + R. \tag{1}$$

Introducing RC ($R = \mathrm{RC} \times P$) and substituting P with R/RC in Eq. 1, we can calculate the ratio of surface runoff depth to infiltration (subsurface runoff) depth as a function of RC:

$$R/F = \mathrm{RC}/(1 - \mathrm{RC}). \tag{2}$$

In this study, we assumed that the bedrock is close to the surface and that all infiltrated water is SSF and does not contribute to groundwater. In the steady-state condition with excess rainfall intensity (I_e) on a hillslope, the maximum surface and subsurface flow (Q_s and Q_{sub}, respectively) can be calculated as (Akan and Houghtalen 2003):

$$Q_s = I_e \times A, \tag{3}$$

and

$$Q_{sub} = I_f \times A, \tag{4}$$

where: I_f is the recharge rate into the soil layer and A is the contributing area of the hillslope. The ratio (m) of the SF peak to the SSF peak can be calculated as:

$$m = \frac{Q_s}{Q_{sub}} = \frac{I_e \times A}{I_f \times A} = \frac{I_e}{I_f}, \tag{5}$$

or:

$$m = \frac{I_e}{I_f} = \frac{R}{F}, \tag{6}$$

where: R is surface runoff depth and F is infiltration depth. From Eq. 2, we have ratio of the SF peak to the subsurface flow peak as a function of RC, so:

$$m = \frac{Q_s}{Q_{sub}} = \frac{\mathrm{RC}}{(1 - \mathrm{RC})}. \tag{7}$$

Based on Eq. 3, we can calculate the coefficients m and RC if we know peak discharge as SSF and SF. In the next step, we need to validate Eq. 3 to investigate the relationship between RC and SF and SSF.

Assuming that base flow is zero. Based on total observed flow ($Q = Qs + Q_{sub}$), Q_s and Q_{sub} are calculated as follows:

$$\begin{aligned} Q_s &= \mathrm{RC} \times Q, \\ Q_{sub} &= (1 - \mathrm{RC}) \times Q. \end{aligned} \tag{8}$$

Thus using Eq. 8, SF and SSF can be calculated separately. In this study, the results obtained using Eq. 8 were validated using the results of laboratory rain simulations on artificial slopes.

As aforementioned, the most important innovation of this study is that the separation of SF from SSF, according to Eq. 8 is based on the runoff coefficient. RC was calculated only from the observed surface flow. In this research, two laboratory models and observed subsurface flow and observed surface flow were used to evaluate Eq. 8.

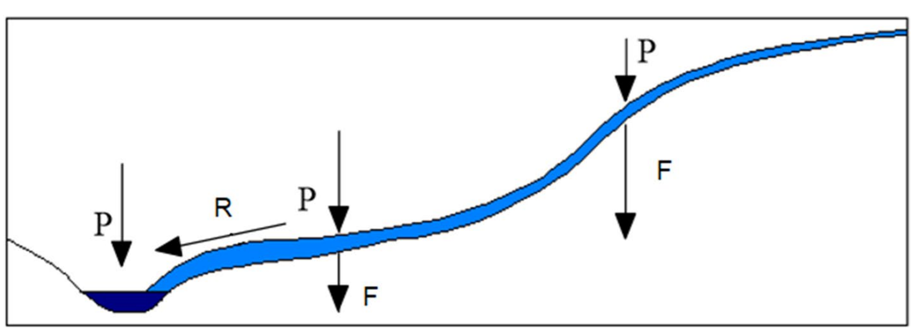

Fig. 1 Schematic diagram of the rainfall-runoff process in a hillslope, where P is precipitation, F is infiltration, and R is surface runoff (Tarboton 2003)

Calculation of runoff coefficient (RC)

Runoff coefficient is the percentage of rainfall that is converted to runoff. Calculation of RC is complex due to the heterogeneity of infiltration across catchments, and in practice, it is impossible to provide an average RC for a catchment. For small hillslopes, we can calculate the average RC by measuring total runoff from the hillslope, using one of the following two methods:

Method (1) RC is calculated as:

$$\mathrm{RC} = V/(P \times A), \tag{9}$$

where: V is runoff volume (i.e., the area below the graph of surface runoff hydrograph) and P is rainfall depth.

Method (2) The RC value is obtained by the rational method, used to predict the runoff peak of small basins, and it is calculated as:

$$\mathrm{RC} = Q_p/(0.278 \times i \times A), \tag{10}$$

where: Q_p is peak surface runoff ($m^3\ s^{-1}$), i is rainfall intensity ($mm\ h^{-1}$), and A is basin area (km^2). It is noteworthy that this method is less accurate than method 1.

Relationship between rainfall and RC

In general, greater amounts of rainfall and lower infiltration rates lead to higher surface runoff or higher RC values.

The SCS-CN infiltration method calculates RC (=R/P) using the following equation (Mishra and Singh 2013):

$$\mathrm{RC} = R/P = \left[(P - 0.2 \times S)^2/(P \times (P + 0.8 \times S)) \right], \tag{11}$$

where: P is rainfall depth in inches and S is potential maximum retention, which is equal to (1000/CN-10), where CN is the selected curve number based on land use, group (from A, sand, to D, clay) and antecedent moisture conditions (from I, dry soil, to III, wet soil) (Chow et al. 1962).

Figure 2 shows the change in RC as a function of change in rainfall intensity from 31.73 to 63.46 mm h^{-1} for a 3-h rainfall event for different values of CN based on Eq. (11).

The CN range for soils with high, medium, and low permeability is 10–30, 40–60, and 70–90, respectively, which directly influences RC. For example, a 20 mm increase in rainfall leads to an increase of around 25%, 15%, and 3% in RC for high, medium, and low permeability soils, respectively.

Effect of slope on RC

Slope is another influential parameter on surface runoff and infiltration (Ribolzi et al. 2011; Morbidelli et al. 2015, 2018). In general, with steeper ground slope, the potential for infiltration is lower and consequently the amount of surface runoff generated will be higher (RC increase).

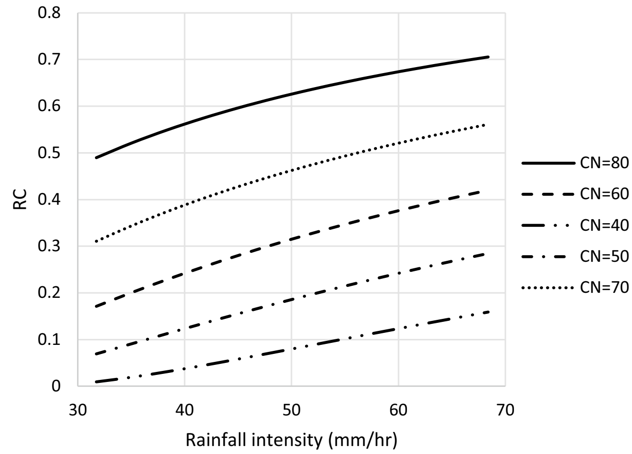

Fig. 2 Relationship between rainfall intensity and RC for different CN values

Table 1 presents the RC values for different types of soils and land uses on different slopes (Liu and De Smedt 2004).

The runoff coefficient for different slopes can be calculated as (Liu and De Smedt 2004):

$$C = C_0 + \left(1 - C_0\right) \times \left(S/\left(S + S_0\right)\right), \tag{12}$$

where: C is RC for slope S % and C_0 is RC for horizontal slope S_0 (0%), which is calculated from Table 2.

Physical model description

Laboratory tests were conducted using an experimental setup at the Hydraulic Laboratory of the Civil Engineering Department at Estahban Azad University, Iran (Fig. 3). It consists of a rainfall simulator over a soil box (length 1.92 m, width 1 m, depth 35 cm, which was filled with loamy sand soil and sandy clay soil. Tests were run with four slopes (0, 3, 6, and 9 degrees) and three rainfall intensities (31.73, 47.6, and 63.46 mm/ h). The rainfall duration in the most event has been about 300 min. Each test has been tested after drying the soil that soil moisture error does not affect measurements. Nozzles tested the intensity of rainfall before each test. SF and SSF were measured by two separate weirs.

Table 1 Effect of slope and land use on RC (Liu and De Smedt 2004)

Land use	Slope (%)	Sand	Loamy sand	Sandy loam	Loam	Silt loam	Silt	Sandy clay loam	Clay loam	Silty clay loam	Silty clay	Clay
Forest	< 0.5	0.03	0.07	0.10	0.13	0.17	0.20	0.23	0.27	0.33	0.37	0.40
	0.5–5	0.07	0.11	0.14	0.17	0.21	0.24	0.27	0.31	0.37	0.41	0.44
	5–10	0.13	0.17	0.20	0.23	0.27	0.30	0.33	0.37	0.43	0.47	0.50
	> 10	0.25	0.29	0.32	0.35	0.39	0.42	0.45	0.49	0.55	0.59	0.62
Grass	< 0.5	0.13	0.17	0.20	0.23	0.27	0.30	0.33	0.37	0.43	0.47	0.50
	0.5–5	0.17	0.21	0.24	0.27	0.31	0.34	0.37	0.41	0.47	0.51	0.54
	5–10	0.23	0.27	0.30	0.33	0.37	0.40	0.43	0.47	0.53	0.57	0.60
	> 10	0.35	0.39	0.42	0.45	0.49	0.52	0.55	0.59	0.65	0.69	0.72
Crop	< 0.5	0.23	0.27	0.30	0.33	0.37	0.40	0.43	0.47	0.53	0.57	0.60
	0.5–5	0.27	0.31	0.34	0.37	0.41	0.44	0.47	0.51	0.57	0.61	0.64
	5–10	0.33	0.37	0.40	0.43	0.47	0.50	0.53	0.57	0.63	0.67	0.70
	> 10	0.45	0.49	0.52	0.55	0.59	0.62	0.65	0.69	0.75	0.79	0.82
Bare	< 0.5	0.33	0.37	0.40	0.43	0.47	0.50	0.53	0.57	0.63	0.67	0.70
Soil	0.5–5	0.37	0.41	0.44	0.47	0.51	0.54	0.57	0.61	0.67	0.71	0.74
	5–10	0.43	0.47	0.50	0.53	0.57	0.60	0.63	0.67	0.73	0.77	0.80
	> 10	0.55	0.59	0.62	0.65	0.69	0.72	0.75	0.79	0.85	0.89	0.92

Table 2 RC values for different land uses and soil types on land with zero slope (*source*: Liu and De Smedt 2004)

Land use	Sand	Loamy sand	Sandy loam	Loam	Silt loam	Silt	Sandy clay loam	clay loam	Silty clay loam	Sandy clay	Silty clay	Clay
Forest	0.680	0.650	0.620	0.590	0.560	0.530	0.500	0.470	0.440	0.410	0.380	0.350
Grass	0.580	0.551	0.522	0.493	0.464	0.435	0.405	0.376	0.347	0.318	0.289	0.260
Crop	0.500	0.471	0.442	0.413	0.384	0.355	0.325	0.296	0.267	0.238	0.209	0.180
Bare soil	0.420	0.393	0.365	0.338	0.311	0.284	0.256	0.229	0.202	0.175	0.147	0.120

Fig. 3 Physical soil model and rainfall simulator used in laboratory tests

Results and discussion

Hydrograph produced by the physical model

For loamy sand soil, the maximum SF measured at the outlet of the physical model varied between 0.78–0.89, 1.31–1.39, and 1.76–1.89 l min^{-1} for the 31.73, 47.6, and 63.46 mm h^{-1} rainfall events, respectively (Fig. 4a–c). The maximum SSF ranged between 0.112 and 0.228 l min^{-1} (Table 3). Substituting the maximum values of observed SF and SSF into Eq. 7 allowed us to calculate RC of the loamy sand (Table 3) for different rainfall events and slopes (Table 4). The observed and calculated runoff coefficient showed a significant positive correlation ($R^2=0.93$) (Fig. 5a).

Table 3 shows the maximum SF and SSF, SF to SSF ratio, calculated RC (Cc) and observed RC (Co) according to the surface runoff volume method.

In tests with loamy sandy soil, the observed RC initially increased with increasing slope, e.g., at a slope of 3 degrees above the horizontal (0 degrees), it increased by about 12% on average (Table 3). However, a further increase in slope from 3 to 6 degrees and from 6 to 9 degrees gave little change in RC. The average increase in SF with an increase in rainfall intensity from 31.73 mm h^{-1} to 47.6 and 63.46 mm^{-1} was between 6.5 and 8.5%. The RC depended on soil type, slope, and land use in our results and was weakly related to rainfall intensity in different events. Thus in practice, it was impossible to calculate RC accurately.

The observed data for sandy clay soil were similar to those for loamy sand soil (Table 3; Fig. 5b). The calculated and observed RC values for the sandy clay were lower than those for the loamy sand, because of the higher permeability of the sandy clay. At 0 degrees of slope, all rainfall contributed to subsurface flow for the sandy clay, and thus the RC is not shown in Table 3. At 6 degrees of slope, the RC increased by 28% and 8% for a rainfall intensity of 47.6 and 63.4 mm h^{-1}, respectively (Table 3). Increasing the rainfall intensity also led to increasing RC for the sandy clay, for instance for a slope of 6 degrees, the RC for a rain intensity of 31.7, 47.6, and 63.46 mm h^{-1} was 0.36, 0.53, and 0.59, respectively (Table 4).

The results of tests in the physical model for two different soils clearly confirmed that the method developed in this study can be recommended as suitable and simple approach to separate SF and SSF in rainfall-runoff analysis of hillslopes. As shown, different parameters, e.g., soil type, land use, slope, and rainfall intensity, influenced the RC value.

Verification based on observed and calculated SSF and SF

In this section, for more accurate validation of the proposed method, surface and subsurface flow information of the other two different soils were used. The first soil was clay loam, and this soil was evaluated by the device according to Fig. 3. The second soil was loamy, and SF and SSF information was examined based on Morbidelli et al. (2015) study.

For first verification of the method, we compared the observed and calculated SSF and SF values obtained for different rainfall rates and slopes (Table 4). For this, we filled the soil box in the physical model (Fig. 3) with a clay loam soil and applied three different rainfall intensities (15.63, 31.3, and 46.9 mm/h). For this experiment, the RC for a slope of 3, 5, and 10 degrees was 0.61, 0.67, and 0.79, respectively.

Figure 6 illustrates the estimated versus observed SF and SSF values. The correlation coefficient of predicted SF in this experiment was 0.972, which is good, and the correlation coefficient of predicted SSF was 0.675, which is acceptable.

Surface flow measurement is recorded more accurately in laboratory models, but there is more error in measuring subsurface flow due to soil moisture storage and the influence of other factors, and this circumstance could have reduced the correlation coefficient in subsurface flow.

Moving from laboratory scale to real catchment scale, usually the lack of observed SSF data is the main obstacle to validating SSF forecasting models. Available SSF data in the hillslope dimension are generally used to validate models (Tiefan et al. 2005; Brown et al. 1999; Ameli et al. 2015; Fariborzi et al. 2019). For a more accurate validation of the method proposed in this study, rainfall simulator data reported by Morbidelli et al. (2015) were used (Table 5). Their data were obtained used a soil box measuring 152 × 122 × 78 cm in length, width, and thickness, respectively, and containing loamy soil. The slope of the box was adjustable from 0 to 10 degree. Table 5 shows the

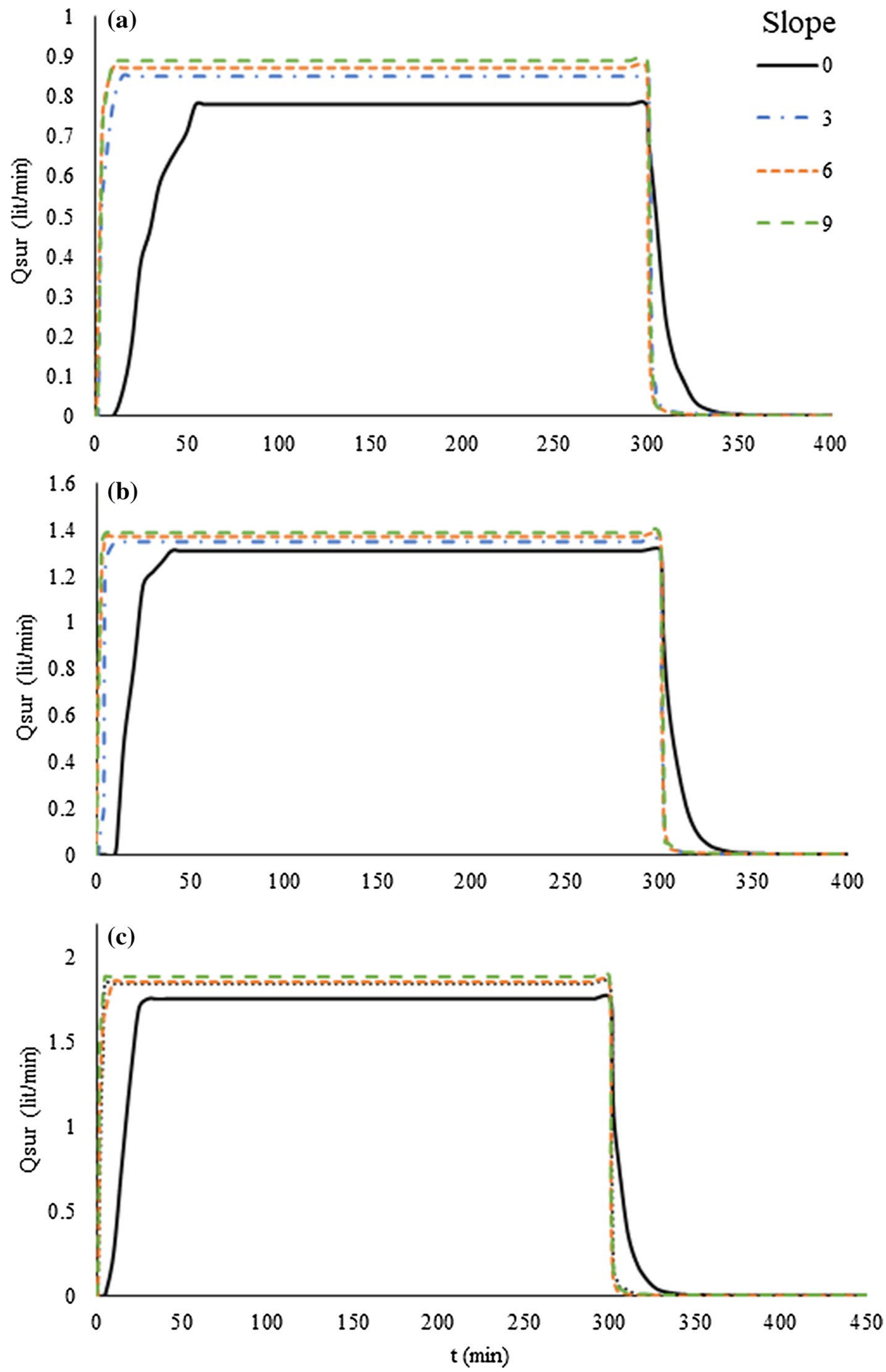

Fig. 4 Observed SF from the physical model with loamy sand soil with different land slope (0–9 degrees) at rainfall intensity of **a** 31.73 mm h^{-1}, **b** 47.6 mm h^{-1}, and **c** 63.46 mm h^{-1}

observed SF and SSF values for different rainfall rates and two slopes, 5 and 10 degrees. For instance, the calibrated values for RC were 0.53 and 0.65 for slopes of 5 and 10 degrees, respectively. The SF and SSF values were also calculated using our method (Eq. 8) (Table 6), and the results were compared with observed maximum SF and SFF reported by Morbidelli et al. (2015). In this case, the correlation coefficient of SF prediction values was 0.93, which is a very good value, and that of SFF prediction values was 0.64, which is acceptable (Fig. 7).

The results showed that the correlation coefficient for predicted SF in this experiment was greater than 0.97, which is very good, and that for predicted SSF was 0.635, which is acceptable.

Table 3 Observed and calculated value of RC based on observations of SF and SSF obtained in a physical model with loamy sand and sandy clay soil

Type of soil	Rainfall intensity (mm h^{-1})	Slope (°)	SSF max (l min^{-1})	SF max (l min^{-1})	SF/SSF	Calculated RC Equation 7 (C_C)	Observed RC Equation 9 (C_o)
Loamy sand	31.73	0	0.214	0.78	3.64	0.784	0.768
		3	0.116	0.85	7.33	0.880	0.836
		6	0.112	0.87	7.77	0.886	0.856
		9	0.112	0.89	7.95	0.888	0.876
Loamy sand	47.6	0	0.224	1.31	5.85	0.854	0.859
		3	0.129	1.35	10.47	0.913	0.886
		6	0.130	1.37	10.54	0.913	0.899
		9	0.114	1.39	12.19	0.924	0.912
Loamy sand	63.46	0	0.228	1.76	7.72	0.885	0.866
		3	0.132	1.85	14.02	0.933	0.910
		6	0.135	1.86	13.78	0.932	0.915
		9	0.114	1.89	16.58	0.943	0.930
Sandy clay	31.73	0	0.500	0.00	0.00	–	–
		3	0.500	0.00	0.00	0.00	0.00
		6	0.320	0.18	0.56	0.36	0.36
		9	0.270	0.23	0.85	0.46	0.46
Sandy clay	47.6	0	1.00	0.00	0.00	–	–
		3	0.60	0.40	0.67	0.40	0.39
		6	0.47	0.53	1.13	0.53	0.50
		9	0.45	0.55	1.22	0.55	0.55
Sandy clay	63.46	0	1.50	0.00	0.00	–	–
		3	0.62	0.88	1.42	0.59	0.58
		6	0.55	0.95	1.73	0.63	0.63
		9	0.50	1.00	2.00	0.67	0.66

Table 4 Observed and calculated SSF and SF for a clay loam soil

Rainfall (Mm h^{-1})	Slope (°)	Observed (l min^{-1})		Calculated (l min^{-1})		SF(PE)	SFF(PE)
		SSF	SF	SSF	SF		
15.63	3	0.5	0.200	0.195	0.305	0.53	0.61
15.63	6	0.29	0.210	0.165	0.335	0.60	0.43
15.63	9	0.24	0.259	0.105	0.395	0.53	0.56
31.3	3	0.58	0.420	0.390	0.610	0.45	0.33
31.3	6	0.4	0.600	0.330	0.670	0.12	0.18
31.3	9	0.39	0.610	0.210	0.790	0.30	0.46
46.9	3	0.58	0.920	0.490	1.000	0.09	0.16
46.9	6	0.45	1.050	0.390	1.110	0.06	0.13
46.9	9	0.43	1.070	0.190	1.300	0.21	0.56

SF(PE) is SF peak error, *SFF(PE)* is SFF peak error

Predicting the SF and SSF hydrograph at catchment scale

Separation of SF hydrograph and SSF hydrograph from observed flood hydrograph is very important for hydrologists. In the previous sections, we focused on separating SF and SF peaks of hillslopes in the laboratory. However, in this section, the proposed RC method was applied to evaluate the separation method in the catchment scale. For further model verification, data on peak SF and SSF from the Heng-Chi and San-Hsia catchments in northern Taiwan were used (Fig. 8; Table 6). The Heng-Chi catchment ranges in elevation from 20 m at the outlet to 970 m and occupies an area of 53.23 km^2, which is covered by forest (70%), cultivated land (25%), and urban area (5%). The San-Hsia catchment is similar, with elevation ranging between 30 and 1770 m and

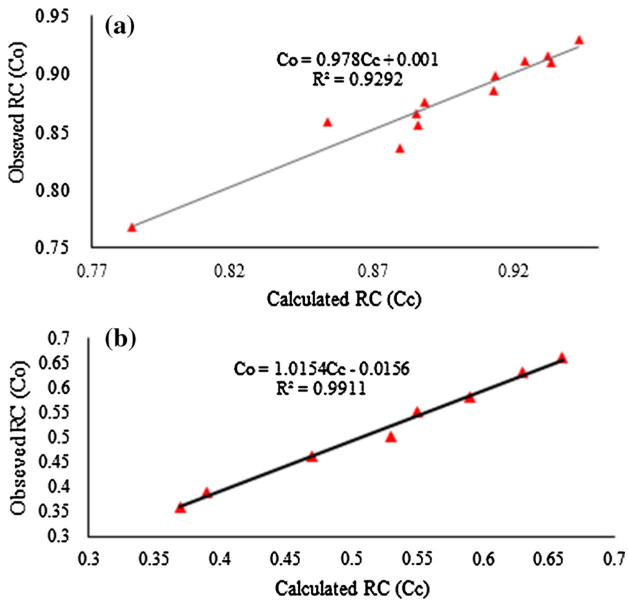

Fig. 5 Correlation between calculated and observed RC for **a** loamy sand and **b** sandy clay soil

area 125.88 km^2, with 75% forest, 20% cultivated land, and 5% urban land use.

Subsurface GIUH model

Chang and Lee (2005) revised the GIUH model to estimate SSF in catchments. In this model, the Darcy's law was adopted to estimate the runoff travel time in subsurface-flow regions. Based on the Horton–Strahler ordering law, any catchment of order Ω can be divided into a series of runoff states. The catchment hydrologic response can be considered to be functions of the runoff path probabilities and runoff travel time probabilities in different runoff states (Rodriguez-Iturbe and Valdes 1979).

Let x_{o_i} denotes the ith-order overland-flow regions in catchment, x_{sub_i} denotes the ith-order subsurface-flow regions, and x_i denotes the ith-order channels, in which $i = 1, 2, \ldots, \Omega$. Ω is maximum order of catchment. The subsurface IUH can be expressed analytically by (Lee and Chang 2005):

$$u_{\text{sub}}(t) = \sum_{w_{\text{sub}} \in W_{\text{sub}}} [f_{x_{\text{sub}}}(t) \times f_{x_i}(t) \times f_{x_j}(t) \times \cdots \times f_{x_\Omega}(t)]_{w_{\text{sub}}} P(w_{\text{sub}}), \tag{13}$$

Fig. 6 Correlation between **a** observed and calculated SSF and **b** observed and calculated SF for a clay loam soil

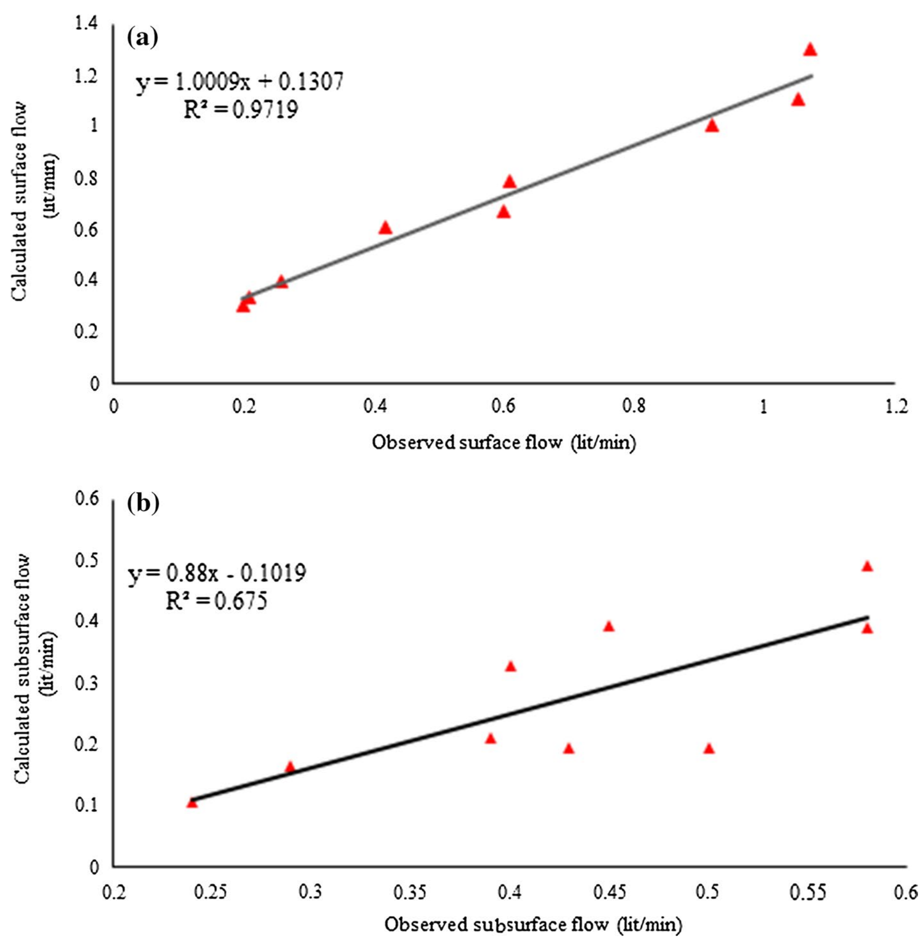

Table 5 Observed and calculated surface flow (SF) and subsurface flow (SSF) (observed) in tests in a physical model (data from Morbidelli et al. 2015)

Slope (°)	Total flow (mm h^{-1})	Observed SF (mm h^{-1})	Observed SSF (mm h^{-1})	Calculated SF (mm h^{-1})	Calculated SSF (mm h^{-1})	SF(PE)	SFF(PE)
5	6.62	4.04	2.58	3.97	2.65	0.02	0.03
5	9.22	5.92	3.3	4.89	4.33	0.17	0.31
5	9.59	5.37	4.22	5.75	3.84	0.07	0.09
5	10.55	5.98	4.57	5.59	4.96	0.07	0.09
5	11.59	7.67	3.92	6.76	4.83	0.12	0.23
10	6.05	3.88	2.17	3.93	2.12	0.01	0.02
10	8.93	6.94	1.99	5.80	3.13	0.16	0.57
10	10.9	8.93	1.97	8.72	2.18	0.02	0.11
10	12.26	10.34	1.92	9.81	2.45	0.05	0.28
10	11.71	9.73	1.98	9.37	2.34	0.02	0.03

SF(PE) is SF peak error, *SFF(PE)* is SFF peak error

Table 6 Recorded SF, peak SF and SSF estimates obtained using the GIUH method, for the Heng-Chi and San-Hsia catchments in northern Taiwan (*source*: Chang and Lee 2008)

Catchment	Event date	DRH (GIUH method)		SF (GIUH method)		SSF (GIUH method)	
		Q_p ($m^3\ s^{-1}$)	T_p (h)	Q_p ($m^3\ s^{-1}$)	T_p (h)	Q_p ($m^3\ s^{-1}$)	T_p (h)
Heng-Chi	08/16/1984	157.8	67	88.8	66	69.3	68
	09/16/1985	587.7	8	553.7	7	34.3	9
	09/17/1986	455.9	41	407.9	40	48.2	43
	07/27/1987	161.5	7	105.5	7	55.9	8
	09/08/1987	318.0	36	238	36	80.0	37
	08/18/1990	486.4	32	476.4	31	10.1	32
	06/05/1993	173.4	11	107	11	66.3	12
	07/10/1994	57.0	12	11	11	45.9	12
	07/30/1996	242.1	30	173	29	68.6	34
	06/22/1997	70.6	5	24	6	47.2	7
	06/18/1999	153.6	4	107	4	47.1	5
	08/22/2000	72.5	18	21	18	52.1	20
	10/31/2000	309.8	18	263	17	46.5	24
San-Hsia	06/03/1983	243.6	14	127	14	116.5	15
	09/16/1985	1449.1	8	1435	8	13.4	9
	07/14/1987	142.1	12	42	11	99.6	15
	07/27/1987	336.5	8	189	8	148.0	9
	08/18/1990	1022.1	31	997	31	25.1	31
	08/30/1990	941.8	16	707	15	234.7	16
	09/07/1990	410.0	25	325	25	85.2	26
	07/10/1994	255.8	13	99	12	156.7	13
	10/09/1994	487.8	20	318	20	170.7	24
	07/30/1996	717.0	31	447	30	270.1	34
	08/17/1997	374.6	32	189	32	185.7	34

where: $u_{sub}(t)$ is subsurface-flow IUH, W_{sub} is the subsurface flow path space given as $W_{sub} = \langle x_{sub_i}, x_i, x_j, \ldots, x_\Omega \rangle$, $P(w_{sub})$ are the probabilities of a raindrop adopting a subsurface flow path of w_{sub}.

In this study, the subsurface GIUH values for these two case study catchments were compared with results obtained using the RC-based model developed in this study.

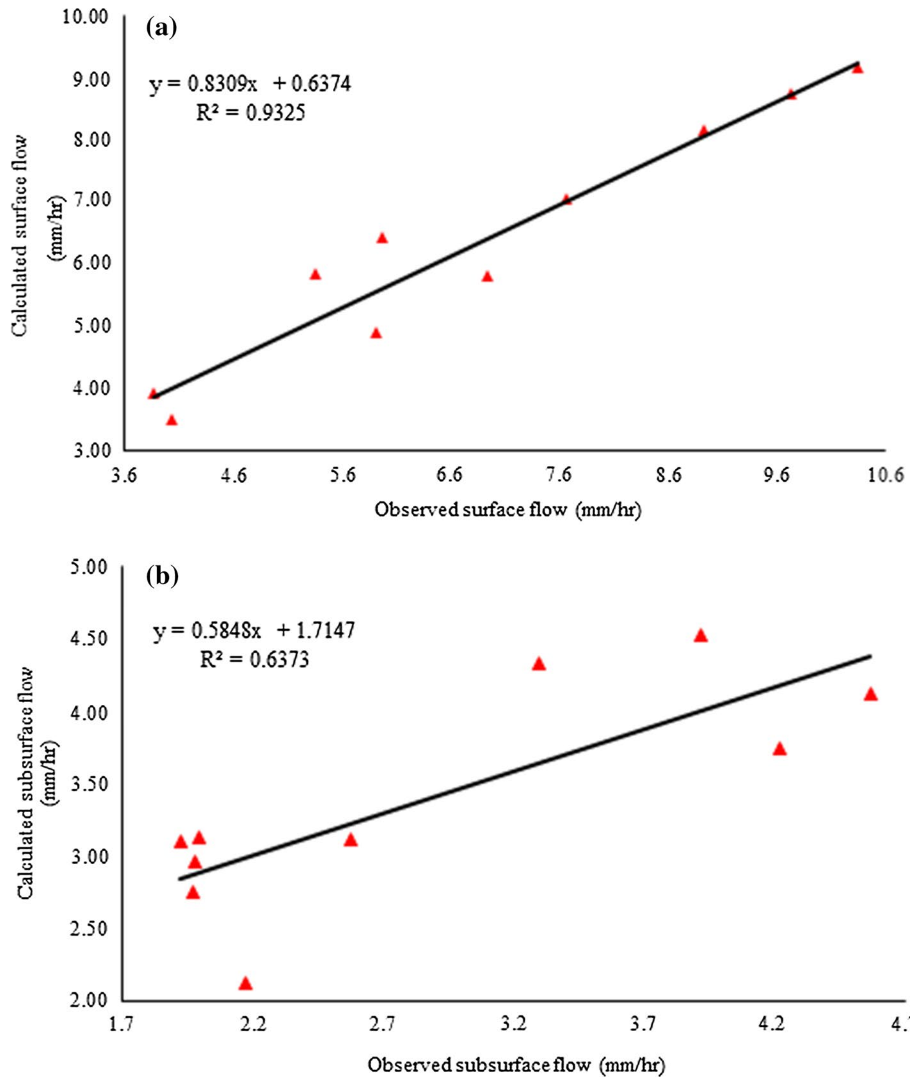

Fig. 7 Correlation between **a** observed and calculated surface flow and **b** observed and calculated surface flow for clay loam soil, based on data in Morbidelli et al. (2015)

In Fig. 9a, the SF values for the catchments calculated using Eq. 8 are compared with the values obtained by the GIUH method in the two catchments recorded by Chang and Lee (2008) (column 3, Table 6). The correlation coefficient was 0.98, which is very good. Figure 9b also shows the SSF values for the two catchments calculated using Eq. 8 and those estimated by the GIUH model. The correlation coefficient in this case was lower, 0.78.

Furthermore, the SSF and SF hydrographs for Heng-Chi (July 1996) and San-Hsia (August 1997) calculated using the GIUH model were compared with those produced using the RC method (Fig. 10). To evaluate model fitness for this purpose, coefficient of efficiency (CE) and relative error in peak (REP) were calculated (Chang and Lee 2008):

$$\mathrm{CE} = 1 - \frac{\sum_{t=1}^{n} [Q_{\mathrm{o}} - Q_{\mathrm{s}}]^2}{\sum_{t=1}^{n} [Q_{\mathrm{o}} - \overline{Q}_{\mathrm{o}}]^2}, \tag{14}$$

$$\mathrm{REP} = 100 \times [Q_{p_{\mathrm{s}}} - Q_{p_{\mathrm{o}}}]/Q_{p_{\mathrm{o}}}, \tag{15}$$

where: Q_{o} is observed discharge at time t; Q_{s} is simulated discharge at time t; $\overline{Q}_{\mathrm{o}}$ is average observed discharge during a storm event; n is number of discharge records during the storm event; $Q_{p_{\mathrm{s}}}$ is peak discharge of the simulated hydrograph; and $Q_{p_{\mathrm{o}}}$ is observed peak discharge.

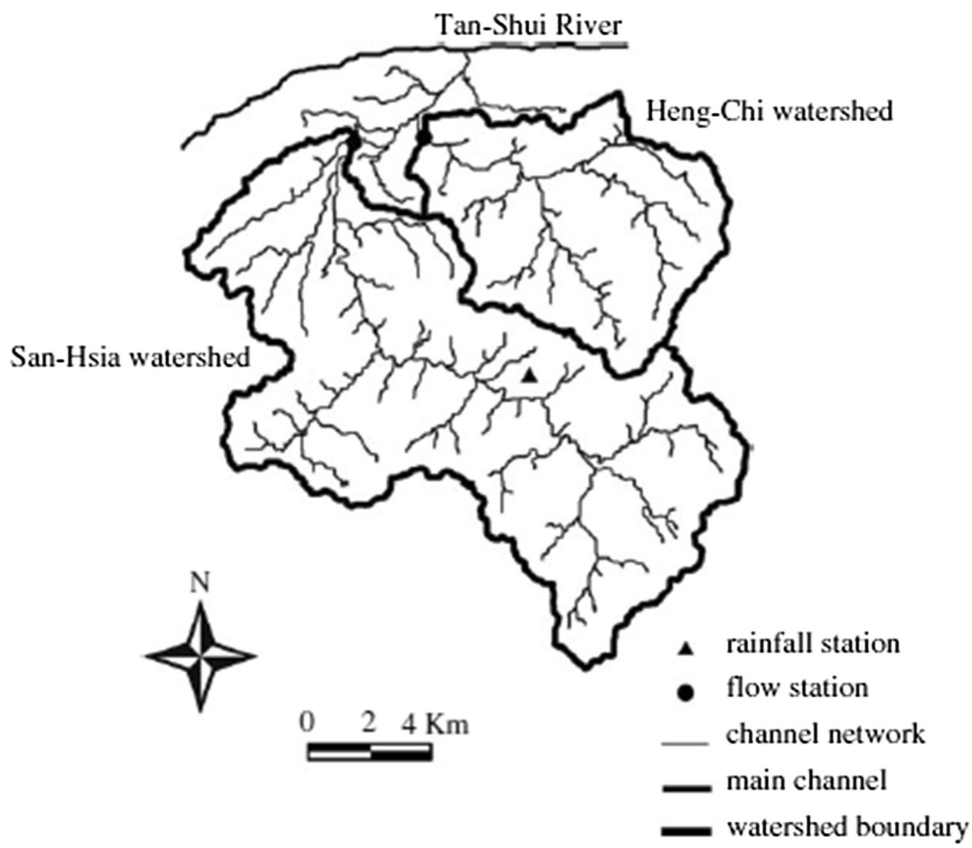

Fig. 8 Location of the Heng-Chi and San-Hsia catchments in Taiwan (after Chang and Lee 2008)

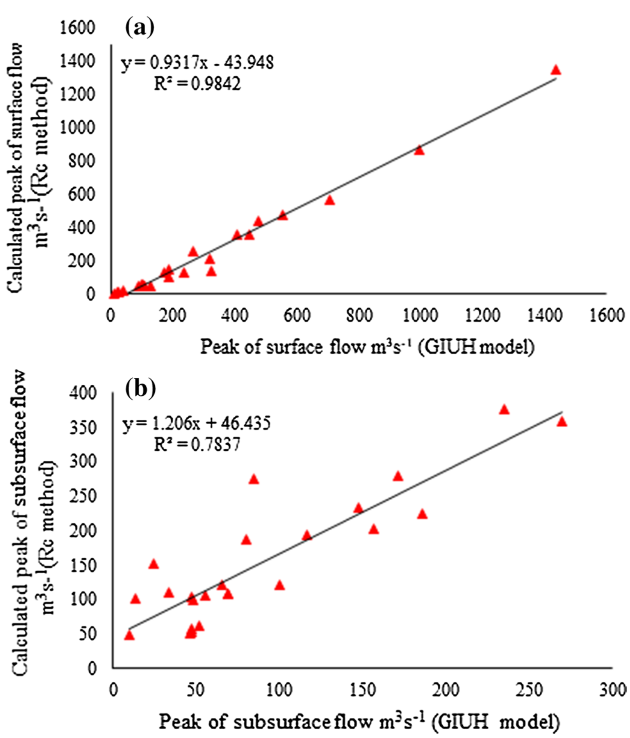

Fig. 9 Comparison of **a** peak SF and **b** peak SFF in Heng-Chi and San-Hsia catchments calculated by the RC method developed in this study and by Chang and Lee (2008) using the GIUH model

The value of CE is between 0 and 1, and CE values above 0.8 are acceptable. The CE was found to be 0.8 and 0.81 for SF, and 0.7 and 0.81 for SSF, in the Heng-Chi and San-Hsia catchment, respectively. Peak error in Heng-Chi was 8% and 80% for SF and SSF, respectively, while it was %18 and %17, respectively, in San-Hsia catchment. Thus, peak error in SSF in Heng-Chi was unacceptably large.

Conclusions

Separation of surface runoff and subsurface runoff from observed data in catchments is difficult, due to the hydrological complexities of runoff. In many permeable catchments with high vegetation cover, subsurface runoff is of great importance. In this study, we applied the concept of runoff coefficient (RC) to devise a simple and practical method for separating surface and subsurface flow in direct runoff from hillslopes or catchments. The accuracy of the method is directly dependent on the accuracy of RC values. We investigated the effect of slope, rainfall intensity, and soil type on RC. Using the SCS-CN infiltration method, we also tested the effect of rainfall intensity on RC for soils with different curve number.

To verify the method, the results were compared with those of laboratory tests on different soils using a rainfall

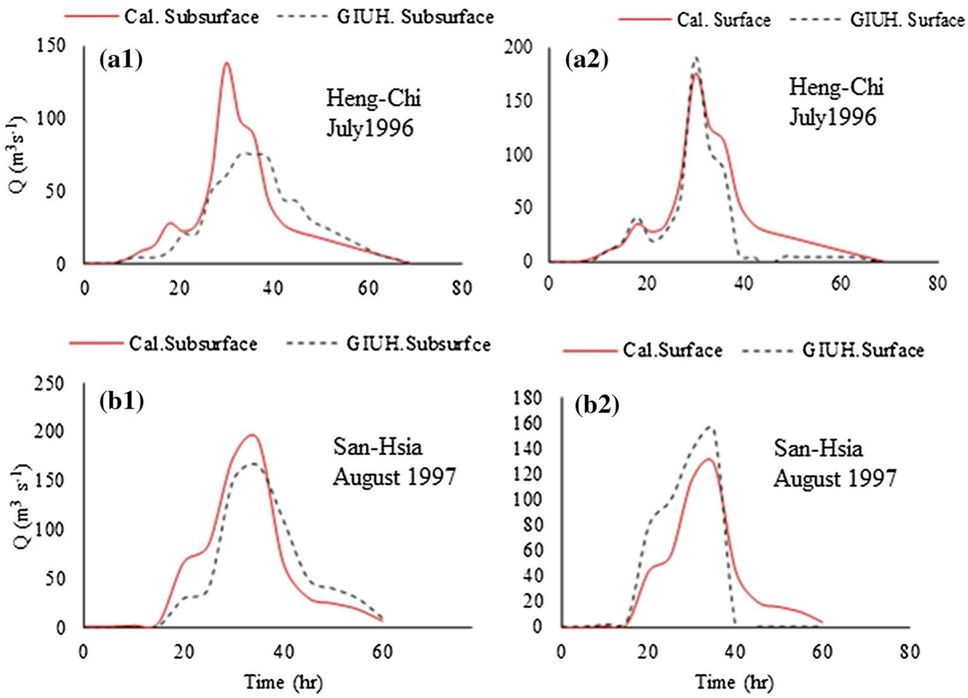

Fig. 10 Hydrographs calculated by the RC method and simulated by the GIUH model for: (1) SF and (2) SSF in **a** Heng-Chi catchment, July 1996 and **b** San-Hsia catchment, August 1997

simulator and an adjustable soil box, and with values predicted by the geomorphological instantaneous unit hydrograph (GIUH) model for two watersheds, Heng-Chi and San-Hsia, in Taiwan. Comparison with laboratory values revealed that our RC-based method accurately predicted peak surface flow and subsurface flow in different soils, with correlation coefficient (CE) 0.93 and 0.65, respectively. GIUH model was used to compare of the surface and subsurface runoff hydrographs of the Heng-Chi and San-Hsia catchments. Based on results, the CE was found to be 0.8 and 0.81 for SF, and 0.7 and 0.81 for SSF, in the Heng-Chi and San-Hsia catchment, respectively. Peak error in Heng-Chi was 8% and 80% for SF and SSF, respectively, while it was %18 and %17, respectively, in San-Hsia catchment. Thus, peak error in SSF in Heng-Chi was unacceptably large. Thus, if RC can be calculated accurately, our method can successfully separate surface and subsurface flow in total runoff.

Acknowledgements This article is based on data in a Ph.D. thesis in Water and Hydraulic Structures (Amin Afshar Ardekani) at Islamic Azad University, Estahban Branch, Fars, Iran.

Declaration

Conflicts of interest The authors declare that they have no conflict of interest.

References

Akan AO, Houghtalen RJ (2003) Urban hydrology, hydraulics, and stormwater quality: engineering applications and computer modeling. Wiley

Ameli AA, Craig JR, McDonnell JJ (2015) Are all runoff processes the same? Numerical experiments comparing a Darcy-Richards solver to an overland flow-based approach for subsurface storm runoff simulation. Water Resour Res 51(12):10008–10028

Brown VA, McDonnell JJ, Burns DA, Kendall C (1999) The role of event water, a rapid shallow flow component, and catchment size in summer stormflow. J Hydrol 217(3–4):171–190

Chang CH, Lee KT (2008) Analysis of geomorphologic and hydrological characteristics in watershed saturated areas using topographic-index threshold and geomorphology-based runoff model. Hydrol Process Int J 22(6):802–812

Chen Z, Govindaraju RS, Kavvas ML (1994a) Spatial averaging of unsaturated flow equations under infiltration conditions over areally heterogeneous fields: 1. Dev Models Water Resour Res 30(2):523–533

Chen Z, Govindaraju RS, Kavvas ML (1994b) Spatial averaging of unsaturated flow equations under infiltration conditions over areally heterogeneous fields 2. Numer Simul Water Resour Res 30(2):535–548

Chow V, Maidment DR, Mays LW (1962) Applied hydrology. J Eng Educ 308:1959

Chow VT, Maidment DR, Mays LW (1988) Applied hydrology. McGraw-Hill, New York

Dehghanian N, Saeid Mousavi Nadoushani S, Saghafian B, Damavandi MR (2020) Evaluation of coupled ANN-GA model to

prioritize flood source areas in ungauged watersheds. Hydrol Res 51(3):423–442
Essig ET, Corradini C, Morbidelli R, Govindaraju RS (2009) Infiltration and deep flow over sloping surfaces: Comparison of numerical and experimental results. J Hydrol 374(1–2):30–42
Fariborzi H, Sabzevari T, Noroozpour S, Mohammadpour R (2019) Prediction of the subsurface flow of hillslopes using a subsurface time-area model. Hydrogeol J 27(4):1401–1417
Foks SS, Raffensperger JP, Penn CA, Driscoll JM (2019) Estimation of base flow by optimal hydrograph separation for the conterminous United States and implications for national-extent hydrologic models. Water 11(8):1629
Harris DM, McDonnell JJ, Rodhe A (1995) Hydrograph separation using continuous open system isotope mixing. Water Resour Res 31(1):157–171
Hursh CR, Brater EF (1941) Separating storm-hydrographs from small drainage-areas into surface-and subsurface-flow. EOS Trans Am Geophys Union 22(3):863–871
Johst M, Casper MC, Muller C, Schneider R (2013) Separation of stormflow hydrographs in surface and subsurface flow by perceptual based modelling of channel inflow components. Open Hydrol J 7(1):66
Keshtkaran P, Sabzevari T, Karami Moghadam M (2018) Estimation of runoff in ungauged catchments using the Nash non-dimensional unit hydrograph. Case study: Ajay and Kasilian catchments
Kim NW, Shin MJ (2018) Estimation of peak flow in ungauged catchments using the relationship between runoff coefficient and curve number. Water 10(11):1669
Kim NW, Shin MJ, Lee JE (2016) Application of runoff coefficient and rainfall-intensity-ratio to analyze the relationship between storm patterns and flood responses. Hydrol Earth Syst Sci Discuss 66:1–48
Lee KT, Chang CH (2005) Incorporating subsurface-flow mechanism into geomorphology-based IUH modeling. J Hydrol 311(1–4):91–105
Lee J, Kwak C, Park H (2015) Estimation of runoff coefficient through infiltration analysis by soil type. J Korean Soc Hazard Mitig 15(4):87–96
Liu YB, De Smedt F (2004) WetSpa extension, a GIS-based hydrologic model for flood prediction and watershed management, vol 1. Vrije Universiteit Brussel, Belgium, p 108
Menberu MW, Torabi Haghighi A, Ronkanen A, Kvaerner J, Kløve B (2014) Runoff curve numbers for peat-dominated watersheds. J Hydrol Eng 20(4):66
Mishra SK, Singh VP (2013) Soil conservation service curve number (SCS-CN) methodology, vol 42. Springer
Morbidelli R, Saltalippi C, Flammini A, Cifrodelli M, Corradini C, Govindaraju RS (2015) Infiltration on sloping surfaces: laboratory experimental evidence and implications for infiltration modeling. J Hydrol 523:79–85
Morbidelli R, Saltalippi C, Flammini A, Govindaraju RS (2018) Role of slope on infiltration: a review. J Hydrol 557:878–886
Petroselli A (2020) A generalization of the EBA4SUB rainfall-runoff model considering surface and subsurface flow. Hydrol Sci J 65(14):2390–2401
Petroselli A, Grimaldi S (2018) Design hydrograph estimation in small and fully ungauged basins: a preliminary assessment of EBA4SUB framework. J Flood Risk Manag 11:S197–S210
Petroselli A, Asgharinia S, Sabzevari T, Saghafian B (2020a) Comparison of design peak flow estimation methods for ungauged basins in Iran. Hydrol Sci J 65(1):127–137
Petroselli A, Piscopia R, Grimaldi S (2020b) Design discharge estimation in small and ungauged basins: EBA4SUB framework sensitivity analysis. J Agric Eng LI:1040
Piscopia R, Petroselli A, Grimaldi S (2015) A software package for the prediction of design flood hydrograph in small and ungauged basins. J Agric Eng XLVI 432:74–84
Ribolzi O, Patin J, Bresson LM, Latsachack KO, Mouche E, Sengtaheuanghoung O, Valentin C (2011) Impact of slope gradient on soil surface features and infiltration on steep slopes in northern Laos. Geomorphology 127(1–2):53–63
Robinson JS, Sivapalan M (1996) Instantaneous response functions of overland flow and subsurface stormflow for catchment models. Hydrol Process 10(6):845–862
Rodriguez-Iturbe I, Valdes JB (1979) The geomorphologic structure of hydrologic response. Water Resour Res 15(6):1409–1420
Sabzevari T (2017) Runoff prediction in ungauged catchments using the gamma dimensionless time-area method. Arab J Geosci 10(6):131
Sabzevari T, Noroozpour S (2014) Effects of hillslope geometry on surface and subsurface flows. Hydrogeol J 22(7):1593–1604
Sabzevari T, Fattahi MH, Mohammadpour R, Noroozpour S (2013) Prediction of surface and subsurface flow in catchments using the GIUH. J Flood Risk Manag 6(2):135–145
Singh VP (1988) Hydrologic systems. Volume I: rainfall-runoff modeling. Prentice Hall, Englewood Cliffs, 480
Tarboton DG (2003) Rainfall-runoff processes. Utah State Univ 1(2):66
Tekeli YI, Şorman Ü (2003) Separation of hydrograph components using stable isotopes case study: the Güvenç Basin, Ankara. Turk J Eng Environ Sci 27(6):383–396
Tiefan P, Jianmei L, Jinzhong L, Anzhi W (2005) A modified subsurface stormflow model of hillsides in forest catchment. Hydrol Process Int J 19(13):2609–2624
Troch PA, Mancini M, Paniconi C, Wood EF (1993) Evaluation of a distributed catchment scale water balance model. Water Resour Res 29(6):1805–1817
Wels C, Cornett RJ, Lazerte BD (1991) Hydrograph separation: a comparison of geochemical and isotopic tracers. J Hydrol 122(1–4):253–274